Experimental Mechanics
DOI 10.1007/s11340-012-9615-3

In Situ Mechanical Testing of Hydrated Biological Nanofibers Using a Nanoindenter Transducer

J. Poissant · F. Barthelat

Received: 1 June 2011 / Accepted: 28 March 2012

Abstract Nanoscale biological fibers, such as collagen, keratin or elastin, serve as building blocks for a wide variety of biological tissues (for example, bone, skin and hair). As such, the elasticity, strength and damage tolerance of these fibers largely control the mechanical performance of tissues at the macroscale. While there is a large body of experimental data for tests on whole biological tissues at the macroscale, mechanical tests on individual biological fibers are scarcer because of their small size (400 nm diameter or less). Isolating, imaging, handling and testing these fibers in hydrated conditions are significant challenges. The AFM-based and MEMS-based techniques developed in the past to test such fibers offer high displacement and load resolution, but they lack the stroke and force capability required to fracture strong and highly extensible fibers such as collagen fibrils. In this work, a microscale mechanical testing platform capable of measuring the tensile stress–strain response of individual type I collagen fibers and fibrils was developed and validated. The platform is composed of a capacitance-based, nanoindenter transducer, an optical microscope to monitor the deformation of the sample *in situ* and a set of micromanipulators to isolate and handle individual fibers and fibrils. Our preliminary results on type I collagen demonstrate the feasibility of monotonic and cyclic tensile tests under the optical microscope and in hydrated conditions. The setup can be used to study the elasticity, strength and damage tolerance of type I collagen fibers and fibrils (using cyclic tests), and our preliminary data are consistent with existing experiments and predictions from numerical models. This setup offers the advantage of being composed from relatively standard components (optical microscope, nanoindenter) which means that it can be easily duplicated in laboratories that already possess these instruments. This technique can be used to assess the effect of environment, genetic diseases or therapeutic drugs on biological tissues at a fundamental level.

Keywords Collagen fibrils · Microtesting platform · Biological material characterization · Damage accumulation · Micro-nanomechanics

J. Poissant · F. Barthelat (✉)
Department of Mechanical Engineering, McGill University, MacDonald Engineering Building, 817 Sherbrooke Street West, Montreal, Quebec H3A 2K6, Canada
e-mail: francois.barthelat@mcgill.ca

J. Poissant
e-mail: jeffrey.poissant@mail.mcgill.ca

Introduction

Proteins are the elementary building blocks of animal tissues. While inherently weak at the molecular scale, their structural organization over multiple, hierarchical length scales leads to robust and multi-functional materials and tissues [1]. A better understanding of the mechanics of protein fibers and fibrils is therefore highly relevant for medicine, tissue engineering or biomimetics. For example, the most common protein is collagen, which is found in all living animal species [2], and which represents the most abundant protein on Earth [3]. Collagen is a major building block of the human body (representing about one third of the total protein content [4]), and provides the structural foundation of bone, cartilage, tendon, tooth dentin, skin, blood vessels and eye cornea [5–8]. A thorough understanding of the mechanics of collagen may lead to improved therapies for osteoporosis and genetic diseases [6, 9]. Collagen is also widely used in tissue engineering to build scaffolds for cartilage or bone reconstruction [10, 11]. In this context, a

Published online: 25 April 2012

better understanding of the mechanical behaviour of collagen is also desirable to optimize the mechanical performance of these scaffolds. Finally, an improved understanding of the construction and mechanics of natural collagen-ceramic composites (such as bone) may inspire new biomimetic designs for engineering composites [12].

Fibrous proteins such as collagen have a well documented structure [13]. At the nanometer length scale, individual collagen molecules (tropocollagen) are formed using three α chains mainly composed of glycine and two other amino acids [4, 5, 13]. The three chains self-assemble by coiling around a common axis, thereby forming tropocollagen molecules. In the most common types of collagen (including type I collagen), tropocollagen molecules self-assemble into long collagen fibrils which have a diameter ranging from 10 nm to 500 nm (depending on the tissue from which it was obtained [14]). The fibril length can range from one to hundreds of microns and multiple fibrils typically assemble into larger scale structures known as collagen fibers.

Experimental techniques for the mechanical characterization of collagenous materials at the tissue level are now well-established in the literature for tendon and fascicles [13, 15–24], for bone [25, 26] and fish scales [27]. However, at smaller length scales the mechanical testing of microscopic collagen fibers and fibrils still presents many challenges: (i) the samples are small (10 nm to 500 nm in diameter for fibrils, which is less than or equal to the wavelength of visible light) and are thus difficult to isolate, visualize, manipulate, position, and attach to a loading device, (ii) the samples must be kept hydrated, which prevents the use of electron microscopes that operate in vacuum chambers and (iii) the force required to rupture a collagen fibril is too low to be accurately measured with conventional load cells, and yet too high for nano and microscale techniques such as force spectroscopy using an atomic force microscope (AFM). Because the force-extension falls into an intermediate regime between macroscale and nanoscale testing, investigations on individual biological fibers such as collagen fibrils are scarce, and are often limited to small deformations [28–33].

Isolating individual collagen fibers and fibrils is typically performed using combined chemical and mechanical disassembly of the macroscale tissue. Chemical procedures can involve digesting non-collagenous materials [34, 35] or swelling the dissected tissue in acid [28, 33]. Mechanical disassembly is often performed using centrifugation [34, 35], blenders [28] or by smearing the collagen tissue on a substrate [33]. Some of these processes may induce severe stress and possibly significant damage on the fibers before they are even tested. The fibers must then be tested in hydrated conditions. Typically, phosphate buffered saline (PBS) is used [28, 33]; however, other researchers have also used moist, ambient air (relative humidity ranging from 30 % to 60 %) [28, 35]. Two approaches have been proposed to test such fibers in tension: microelectromechanical systems (MEMS) loading devices [34, 35] or AFM force spectroscopy [28, 33]; however, both methods have limitations. For example, neither method has yet been shown to fail the sample and therefore obtain the full (up to failure) stress–strain curve for collagen fibrils. Additionally, the MEMS-based device measures displacements using an integrated Vernier scale which limits the resolution to about 0.25 μm [35]. The AFM techniques, on the other hand, typically have excellent resolution of force and displacement; however, their maximum allowable force and displacement are limited so that investigations remain in the small-strain (<5 %) regime [28, 33]. Another important limitation of AFM techniques is that the test is "blind": the sample cannot be imaged as it is stretched *in situ*. Without *in situ* imaging, important information such as the location of sample failure (within the gage region or not) is unavailable.

At smaller length scales, the mechanical response of individual collagen molecules were experimentally studied using Brillouin scattering [36], X-ray diffraction [17], optical tweezers [37, 38] and force spectroscopy [39, 40]. However, without the means of accurately measuring the diameter of the molecule, the mechanical tests have considerable uncertainty. This type of experimental data is also needed to validate and complement recent numerical simulations that have revealed unique mechanisms associated with the molecular structure of these fibers [41, 42].

This article presents an alternative approach to the testing of long biological nanofibers such as type I collagen fibrils. A first section presents the design and validation of an alternative microscale mechanical testing platform. Afterwards, the second section presents the protocol for preparing and handling individual collagen samples (fibers or fibrils). Details on the tensile testing procedures follow in the third section. Finally, preliminary results from type I collagen tensile tests are presented in the last section.

A Capacitance-Based Microscale Testing Platform

Among existing technology for nanoscale actuation and small force measurement, capacitance-based approaches offer a powerful combination of high force capacity, high resolution and sensitivity. Capacitance-based transducers are used in nanoindentation where they offer nanometer and nanonewton resolutions. In this work, we used a commercially available nanoindenter transducer (Hysitron Inc., Minneapolis, MN) used in lateral force (scratch) mode, following the recent work of Kaul and Prakash [43]. In this setup, the Hysitron transducer was used as both the sensor and the actuator for the tensile tests. The transducer consists of a three electrode plate capacitive system, with two outer

electrodes which remain fixed and one inner electrode which is held by springs and is essentially free to float between the outer plates. An AC voltage is applied to the outer electrodes creating a linear electric field between the plates (as in a conventional electric capacitor). The nanoindenter transducer tip is connected to the floating electrode and the electric potential of the floating electrode is used to measure tip displacement. A DC bias, applied to one of the two fixed electrodes, creates an electrostatic attraction with the floating electrode. The stiffness of the springs holding the floating electrode can be calibrated with the magnitude of this DC bias to measure force.

Figure 1 shows an overview of the experimental setup. The transducer was clamped, upside-down, to the stage of an upright optical microscope (Olympus Canada Inc., Markham, ON) which is equipped with a CCD camera (Retiga-2000R, 1600×1200 pixel resolution) that was controlled by an imaging software (QImaging, Surrey, BC). Differential interference contrast microscopy was used to image the fibers. Two micromanipulators (model MX1680R, Siskiyou Inc., Grants Pass, OR and model SP-170X, Signatone Corporation, Gilroy, CA) were mounted on either side of the microscope stage in order to handle samples or to apply small amounts of glue or liquid. The entire setup was placed on a vibration isolation table (model 63–521 TMC, Peabody, MA). One end of the sample was fixed to a substrate which was held by a micromanipulator. The other end was fixed and tested at the edge of a platform made of mounting epoxy, which extended past the side of the transducer (Fig. 1(b)). This platform was mounted on the transducer tip to prevent water from entering the transducer while testing in hydrated conditions.

The accuracy of the nanoindenter transducer was verified (because of its unusual upside-down arrangement) by deflecting a rectangular AFM cantilever of known stiffness with the transducer tip [44]. The stiffness of a rectangular AFM cantilever (tapping mode AFM probes, model MPP 11100–10, Veeco Instruments Inc., Plainview, NY) was first measured using the hydrodynamic technique [45, 46], which has been reported as being at least 10 % accurate compared to other measurement methods [47]. The hydrodynamic technique measured a stiffness of 66 (±7) N/m. The AFM cantilever was then mounted on a micromanipulator and deflected using the nanoindenter transducer tip (in lateral mode) at rates of 0.23 μm/s and 0.70 μm/s, up to 5 microns, and then brought back to its initial position. The load–displacement curve was linear during loading and unloading (Fig. 2), and rate independent. The loading and unloading portions of each curve were fitted with straight lines to yield the stiffness. The average stiffness was found to be 66 N/m with a standard deviation of 4 N/m (44 measurements). This result matched the reference value obtained from the hydrodynamic technique and was within the range of accuracy of similar investigations [44]. Therefore, this test validated the measurements of the upside-down nanoindenter transducer in lateral mode.

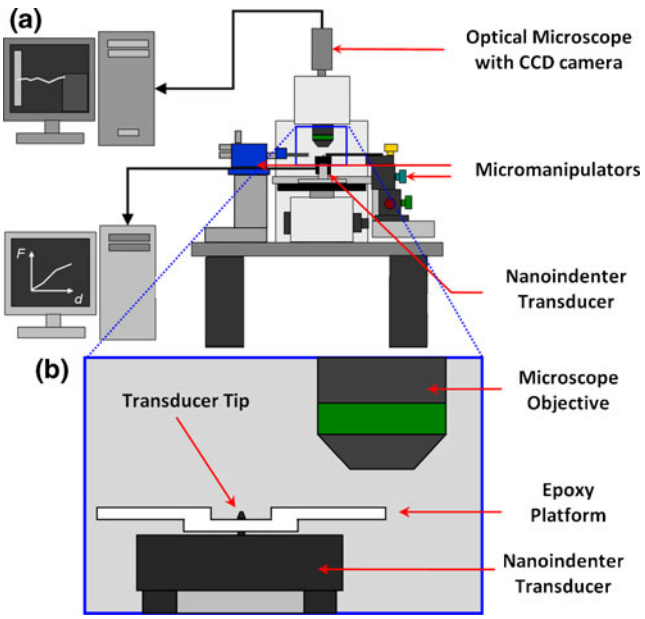

Fig. 1 (**a**) Overall setup of the microtesting platform; (**b**) a closer view of the transducer with an epoxy platform on its tip onto which one end of the sample is fixed

Sample Preparation

The tasks of isolating, handling and testing individual collagen fibrils represent significant challenges that were addressed by developing new experimental protocols, as discussed in this section. The scales of a striped bass (*Morone Saxatilis*) were used as the source of type I

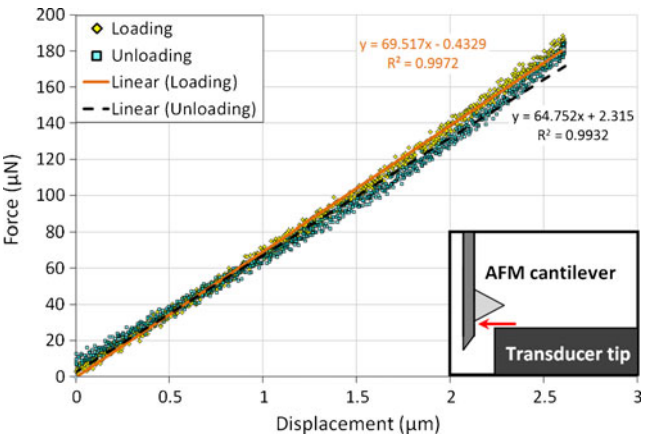

Fig. 2 A representative force-displacement curve obtained when deflecting an AFM cantilever with the transducer tip of the microtesting platform. The inset schematic illustrates the experiment as seen through the microscope

collagen fibrils. These fish scales are about 400 μm thick and are composed of an outer mineralized bony layer and an inner layer made of collagen fibers arranged in a crossply fashion [48]. A whole, fresh, striped bass was purchased from a local fish market and the scales were plucked manually from the skin. The extracted fish scales were stored in a freezer at approximately −20 °C. On the day of testing, a fish scale was thawed at ambient temperature and rinsed with Milli-Q water (highly distilled, deionised water) [33]. Several collagen lamellae were detached and peeled off from the fish scale using two sets of tweezers. The detached collagen lamellae were then torn into smaller and smaller strips using the tweezers, which yielded ribbon-like bundles of collagen fibers (Fig. 3(a)). The ribbons were then deposited onto a glass slide and separated along the fiber direction using the micromanipulators, which exposed a large number of collagen fibers and fibrils (Fig. 3(a)). AFM imaging (Veeco Instruments Inc., Plainview, NY) confirmed that the isolated materials included individual collagen fibrils 200 to 300 nm in diameter with the characteristic 67 nm D-banding pattern [13] (Fig. 3(b)). These "microdissections" were performed in hydrated conditions using thin layers of Milli-Q water. When dry, the collagen ribbons were brittle and could not be smeared, most likely because of hydrogen bonds forming within fibers as the ribbon dried.

Once fibers and fibrils were identified, they were spread over a 10 to 30 μm wide trench formed by two silicon substrates (Fig. 4(a)). A successful dissection yielded several (three or more) individual fibers and fibrils spanning across the gap between the two substrates. An AFM cantilever was then mounted onto one of the micromanipulators and was used to deposit a droplet of epoxy glue (model 8276, J.B. Weld, Sulphur Springs, TX) on one end of each fibril (Fig. 4(b)). As reported in previous work, epoxy was found to have the best adhesion on collagen [35]. A water droplet was added on the other side of the gap to release the fibrils from the substrate (Fig. 4(c)). The two substrates were then slowly moved apart and separated, which resulted in multiple cantilevered fibrils attached to one substrate (Fig. 4(c)). The substrate with the cantilevered fibrils was then positioned near the transducer platform using a micromanipulator, while the free end of one of the fibrils was placed onto the platform. The second micromanipulator, with an AFM tip attached at its end, was used to deposit a droplet of epoxy glue that clamped the free end of the collagen fiber to the platform (Fig. 4(d)). The epoxy was left to cure for 8 h in ambient conditions before starting the tests. In general, it was found that when the ambient relative humidity was greater than 40 %, trace amounts of water deposited on the substrate (as a result of the dissection procedure) would surround the epoxy droplets and the samples (Fig. 5) and would remain on the surface until testing time. Future tests will include the capability to add more water or saline to the substrate during the long curing time to ensure that all samples remain hydrated (especially when ambient humidity levels are low).

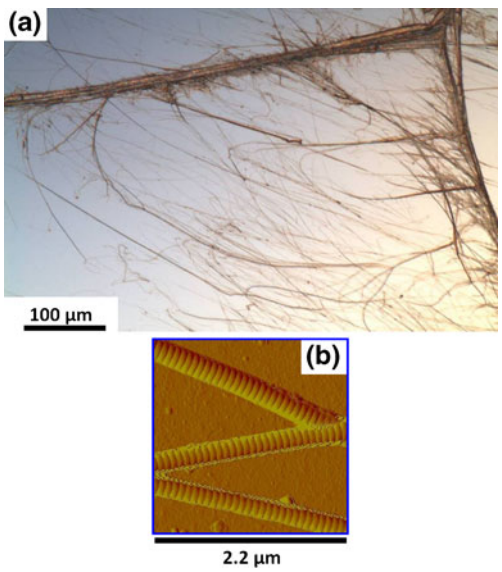

Fig. 3 (**a**) Exposed collagen fibers and fibrils obtained by tearing a ribbon of collagen tissue. (**b**) An AFM scan reveals the approximately 67 nm D-period banding pattern of collagen fibrils

Testing Procedure

In order to stretch the sample, the transducer tip was actuated using displacement-controlled loading functions programmed prior to the actual testing. Load and displacement were recorded by the transducer during the test, while images of the fiber were captured with the optical microscope (Fig. 5). Non-specific loads are forces measured by the transducer which are only due to the stiffness of the transducer itself. These forces were measured as a function of displacement by repeating the programmed tensile test four times after failing the sample (averaging the results) and were then subtracted from the load–displacement data obtained during the sample tensile test. The engineering stress was obtained by dividing the corrected values of tensile force by the initial cross-sectional area of the sample before deformation. The collagen samples were all assumed to have a circular cross-section, and the diameters of collagen fibers (≈1 μm) were measured directly from digital images captured using the optical microscope. Collagen fibril samples were imaged after testing with the AFM to measure their diameters (<500 nm). To account for variations in sample diameter, four measurements were made along the length of the sample and these were then averaged. The variation of diameter for the collagen fibers and fibrils did not exceed ±16 % from the mean diameter. Engineering stress was used instead of true stress because the current experimental setup has no means of accurately tracking the changes in sample cross-section during testing.

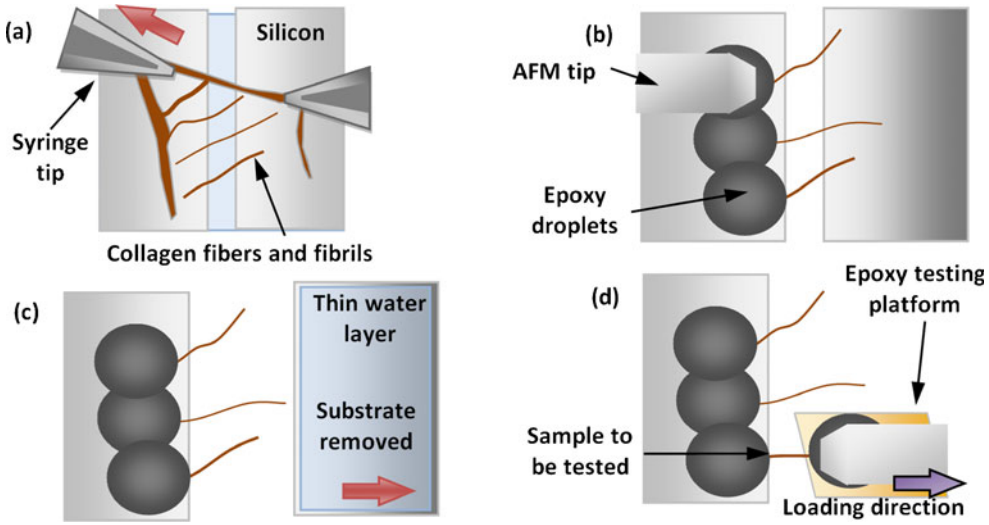

Fig. 4 Handling and testing of individual fibrils: (**a**) collagen ribbons are dissected so that individual collagen fibrils span a trench formed by two silicon substrates. (**b**) An AFM tip is used to apply droplets of epoxy glue on one end of each fibril. (**c**) Water is deposited onto the other fibril ends to release them from their substrate, and the substrate is slowly moved away. (**d**) The free end of the selected sample is glued onto the testing platform. All steps are performed under the optical microscope

The strains in the collagen sample were determined from both the transducer data and from imaging. The displacements measured by the transducer were plotted against the strains computed from the images, which produced a nearly linear curve. The slope of the line-of-best-fit provided an "effective gage length", which was subsequently used to compute the strain from the transducer displacements. The strains were therefore determined accurately, rapidly and in a quasi-continuous fashion. For these preliminary tests, engineering strains were used for their simplicity and to compare with existing results from the literature [35]. Future tests will include direct, on-sample measurements of displacements using optical methods and Lagrangian strains.

Results and Discussion

In this section, the capabilities of the experimental setup developed in this work are demonstrated for individual collagen fibers and fibrils. Figure 6 shows the force-extension and corresponding stress–strain curves obtained for a collagen fiber (diameter: 1.4 μm, effective gage length: 22.5 μm) stretched up to failure at a rate of 0.67 μm/s (engineering strain rate 3.0 %/s). The elastic modulus of

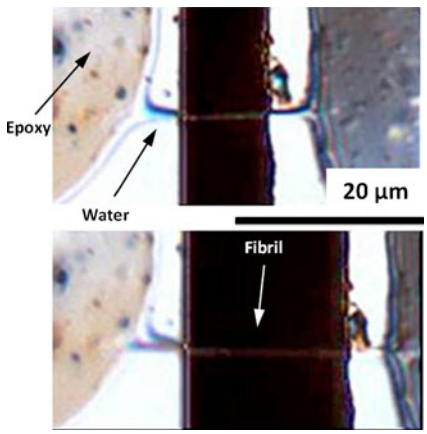

Fig. 5 Two images of a collagen fibril sample acquired during testing

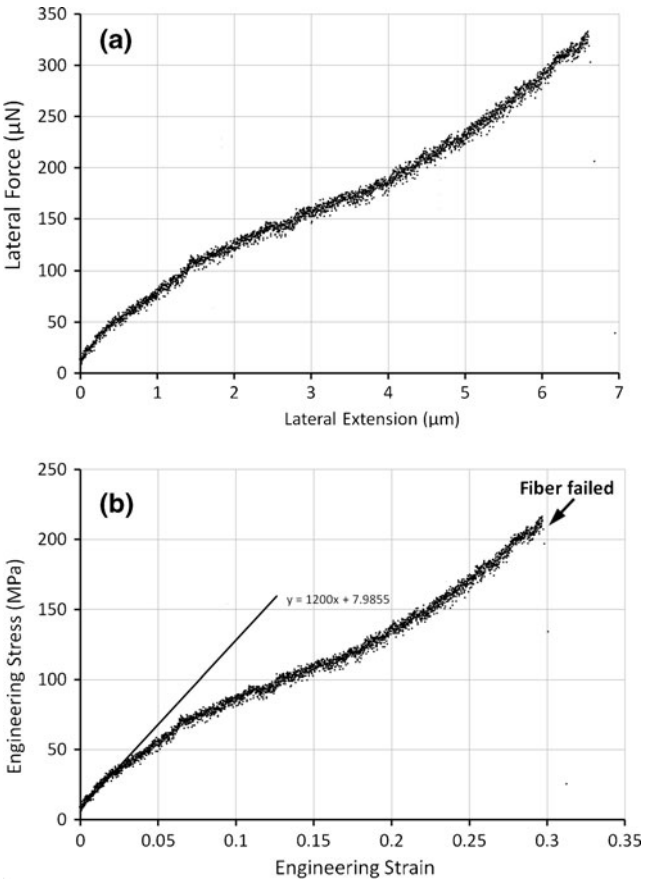

Fig. 6 (**a**) Force-extension curve for tensile test on a collagen fiber. (**b**) Corresponding engineering stress–strain curve

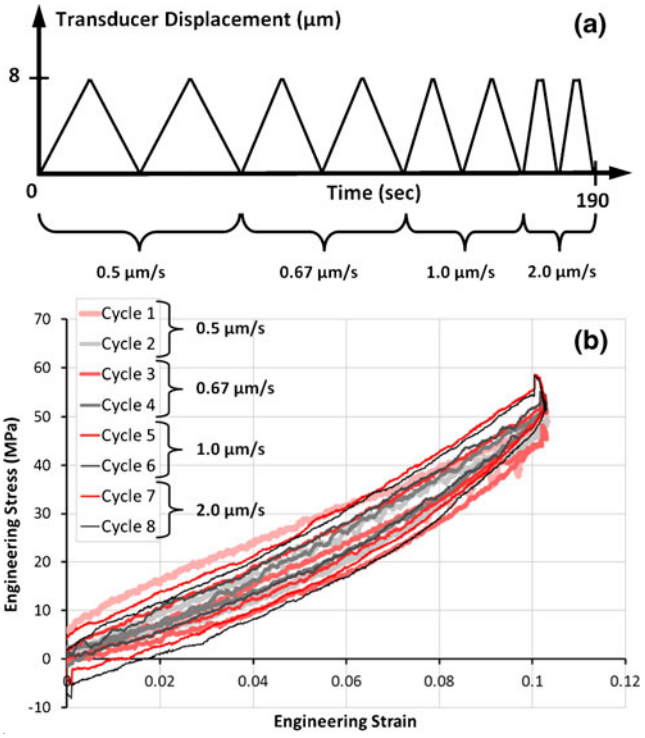

Fig. 7 (**a**) The input loading function for the variable rate cyclic tests. Loading rate was increased after every 2 cycles, up to 8 cycles. (**b**) Resulting cyclic stress–strain curves

the collagen fiber was computed by fitting a line to the initial region of the stress–strain curve (Fig. 6(b)) providing a value of 1.20 GPa, which is within the range of moduli previously measured for collagen fibrils [28, 34, 35]. Additionally, the slope of the stress–strain curve increased in the region just prior to failure. Such strain hardening behaviour has been reported previously for fibrils: as suggested by Shen et al. [35], one possible explanation for the strain hardening behaviour is the movement of water within the sample. The reduction in fiber radius could create internal pressure driving water out of the sample, increasing the number of hydrogen bonds and increasing stiffness. Another possible mechanism was discussed by Gautieri et al. [42] based on results from numerical simulations: when collagen molecules are stretched at rates less than 0.5 m/s (which, according to the authors, represent physiologically and experimentally relevant loading rates), the molecules can unravel and straighten their α chains along the direction of applied load, which also increases stiffness. The fiber eventually failed in tension within the gage region, providing measures of strength and strain at failure of 212 MPa and 30 %, respectively. Additional data and statistics are required to get a more accurate understanding of these mechanical properties and their variations across samples; however, this preliminary test demonstrated the capabilities of the proposed experimental setup. The system is sensitive enough to capture features on the force-extension curve, and at the same time provides sufficient stroke and force to fracture the collagen fiber.

The capability of the system to measure load and displacement in a continuous fashion together with the ease of programming specific loading sequences provides a unique opportunity to examine the viscosity and cyclic behaviour of collagen fibers. To this end, rate effects were explored by performing tensile tests using cyclic loadings of constant amplitude but at increasing load rates. The cyclic tests consisted of eight cycles, each containing four segments: loading, holding at a full extension of 8 microns, unloading, and holding at zero displacement (Fig. 7(a)). The loading rates were increased after each pair of cycles. The sample used for this test was a collagen fiber (diameter: 1.1 μm, effective gage length: 47.7 μm).

The fiber was hydrated from water on its substrate (as in Fig. 5) and demonstrated no signs of permanent plastic deformation, even after undergoing relatively high (10 %) strains (Fig. 7(b)). Shen et al. [35] remarked that fibrils recovered from residual strains at a relative humidity of about 90 % and with 100 min of recovery time. However, the tests performed by Shen et al. were on collagen fibrils instead of fibers, and samples were strained past 10 % [35]. Figure 7(b) demonstrates that humid collagen fibers from fish scales might recover from residual strains on the order of seconds (for strains less than 10 %). The negative stresses in Figure 7(b), which occur at nearly zero strain during unloading segments, indicate that the sample is being slightly compressed. This compression could be the result of loading the sample past its yield point, causing inelastic deformation and an increase in sample length. However, because stress returns to approximately zero at the start of each loading cycle, the fiber appears to have recovered from these residual strains. Further testing would be required to help solidify these preliminary observations.

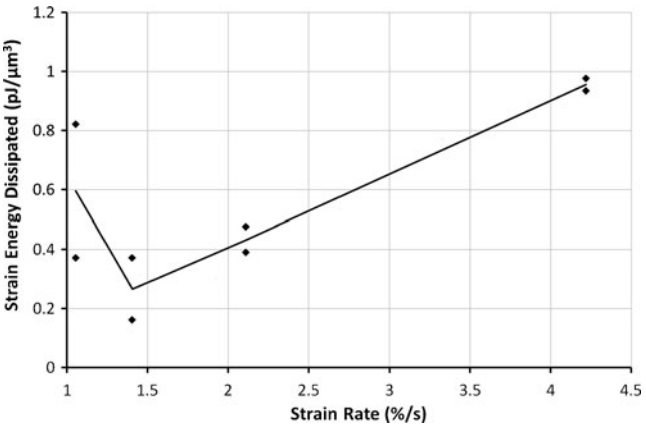

Fig. 8 Strain energy dissipated as a function of strain rate. At each strain rate, two cycles were performed. The upper marker corresponds to the first cycle. The solid line represents the average of the two markers at a given rate.

The amount of strain energy dissipated as a result of viscoelasticity was also quantified by calculating the area of the loading-unloading hysteresis loop on the stress–strain curve. Figure 8 presents the dissipated strain energy versus the strain rates (1.05 %/s, 1.41 %/s, 2.11 %/s and 4.22 %/s). At a given strain rate, two cycles were performed yielding two points on Fig. 8. The average value of each pair was used to obtain the result graphed using solid lines. The results presented on Fig. 8 are consistent with previous experimental results on fibrils [33] whereby increasing the strain rate increases the amount of dissipation. For each pair of cycles, the first cycle consistently dissipated more energy than the second cycle, possibly because intramolecular hydrogen bonds were ruptured during the first cycle and these did not have time to reform for the second cycle (the rupturing and formation of hydrogen bonds is a dissipative process). This rupturing of hydrogen bonds might also explain why the first cycles had much larger differences than later cycles and why the lowest strain rate dissipated more energy than the second lowest.

Cyclic tests can also be used to assess the accumulation of damage in individual collagen fibers and fibrils. In its simplest form, damage is characterized by one damage variable and can be written as follows [49]:

$$D = 1 - S/S_0$$

where S is the current stiffness of the sample and S_0 is the initial stiffness of the undamaged sample. This ratio eliminates the need to measure the initial cross-sectional area (A) and the initial length (L) of the sample. By this definition, damage can vary from D=0 (no damage) to D=1 (complete failure: the material has zero stiffness and cannot sustain any load). In practice, materials typically fail when the damage reaches a critical value, D_c<1. In this work, damage accumulation was studied in an individual collagen fibril (diameter: 0.316 μm, effective gage length: 12 μm) by cyclic load/unload tests of increasing amplitude (Fig. 9(a)). Cyclic loads were performed at a constant rate of 1 μm/s. During the first cycle, the sample was stretched by 3 μm, and at each following cycle the displacement amplitude was increased by 1 μm to progressively induce damage in the sample. The unloading/reloading sequence was used to measure the evolution of modulus and in turn used to compute damage accumulation. The transducer was held stationary for 0.5 s between each loading and unloading segment (during which sample recovery was assumed negligible) in order to prevent rapid changes in transducer acceleration. Figure 9(b) shows the cyclic stress–strain curves resulting from this experiment. Negative stresses are observed for near-zero strains after the unloading portion of the third cycle. These negative stresses are the result of loading the fibril past its yield stress, causing inelastic deformations and an accumulation of residual strains; when the loading stage returns to zero the fibril is slightly compressed. The fibril eventually failed after 7 cycles, at a strain of 58 % and stress of 125 MPa. The stress and strain at failure were lower than the values proposed by Shen et al. for monotonic loading (over 600 MPa and 100 %, respectively [35]) most likely because of the incurred damage from repeatedly loading the fibril past its yield stress. In fact, Shen et al. found that the yield stress of fibrils decreased between cycles after loading/unloading a sample past its yield point [35].

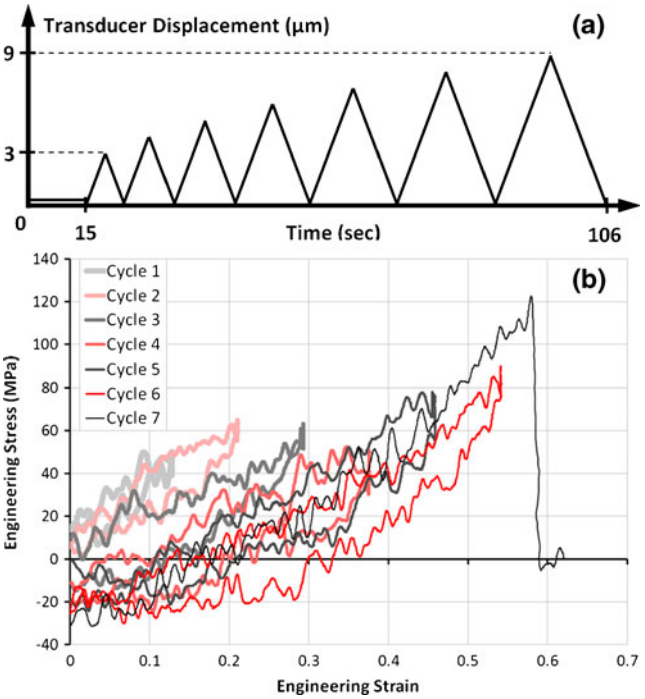

Fig. 9 (**a**) The input loading function for the cyclic tests with variable maximum displacement. Loading/unloading rates were constant at 1 μm/s. (**b**) The resulting stress–strain behaviour for the collagen fibril

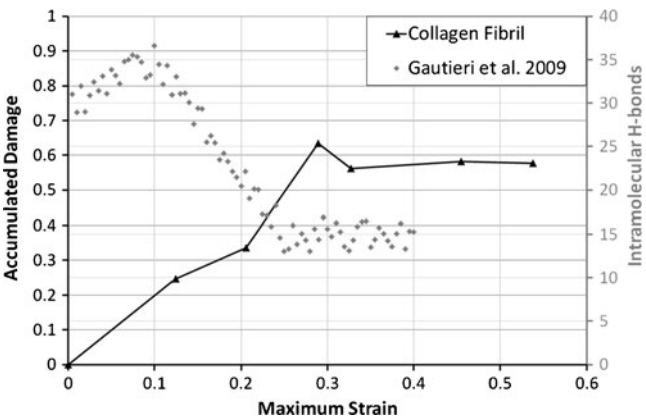

Fig. 10 Damage accumulation versus maximum strain of the previous cycle compared with an approximation of the results presented in Gautieri et al. [42]

The stiffness of the sample was evaluated at the beginning (loading segment) of each cycle using the slope of the line-of-best-fit to the data points comprising the first 3 % strain. This data was used to compute the accumulated damage as a function of maximum strain endured by the fibril (Fig. 10). Damage increases significantly up to 30 % strain, after which no further damage was recorded. Further straining the fibrils causes little additional damage before failure. The maximum amount of damage withstood by the sample was $D_{max} \approx 0.6$. This trend might be explained by the progressive breakage of hydrogen bonds between tropocollagen molecules, which was predicted for a single collagen molecule from numerical simulations [42]. Figure 10 shows that this evolution followed a trend consistent with the damage evolution we measured on a single fibril. The decreased number of intramolecular hydrogen bonds (as measured in molecular tensile test simulations) appears to be directly correlated with the increased damage (or decreased modulus) incurred by the fibril during tensile testing. Similar qualitative trends were observed for 2 other fibrils tested under dry conditions (not shown here for brevity); however, these dry fibrils ruptured at lower maximum strains (between 20 % and 30 % strain). While more experimental data is needed to assess the damage accumulation of collagen fibrils, these preliminary tests demonstrate the versatility of our microscale experimental platform.

Conclusions

In this work, a microtesting platform based on a standard, capacitance-based transducer from a nanoindenter was developed and validated, and its ability to measure the tensile behaviour of nanosclae biological fibers in hydrated conditions was demonstrated. New protocols to mechanically purify collagen fibers and fibrils were developed and presented. To demonstrate the capabilities of the experimental setup, three types of mechanical tests were performed on collagen fibers and fibrils. Preliminary results range from supporting previous measurements to quantifying relevant properties of individual collagen fibers and fibrils: elasticity, strength, rate dependence and damage tolerance. While further testing is required to ensure consistency and to provide conclusive experimental evidence on the mechanical behaviour of individual fibrils, the present results demonstrate the feasibility of these tests and the versatility of the experimental setup. Sample preparation and handling remain the main challenge in this type of testing, which explains the small number of samples tested in this preliminary work. This is consistent with previous experimental work on nanoscale biological fibers, where the number of samples can range from two [33] to just over a dozen [35]. We are currently exploring ways to streamline the preparation process so that a larger number of samples can be tested in a shorter amount of time. The device presented in this work overcomes some of the limitations of MEMS- and AFM-based systems by developing sufficient stroke and force to rupture a collagen fibril (up to failure), while providing high resolution measurements with *in situ* observation. Finally, the setup described in this article was assembled using instruments which are relatively common in research laboratories (optical microscope, nanoindenter, micromanipulators). Thus, it can be duplicated or adapted with relative ease to provide unique opportunities for the testing of micro and nanoscale biological fibers, in hydrated conditions, at a fundamental level.

Acknowledgments The authors would like to thank the Natural Sciences and Engineering Research Council of Canada (NSERC) for supporting this work through an Alexander Graham Bell Canada Graduate Scholarship at the Master's level and a Postgraduate Scholarship Extension at the Master's level.

References

1. Ackbarow T, Buehler MJ (2008) Hierarchical coexistence of universality and diversity controls robustness and multi-functionality in protein materials. J Comput Theor Nanosci 5:1193–1204. doi:10.1166/jctn.2008.001
2. Solomon E, Cheah KSE (1981) Collagen evolution. Nature 291:450–451. doi:10.1038/291450a0
3. Buehler MJ (2008) Nanomechanics of collagen fibrils under varying cross-link densities: atomistic and continuum studies. J Mech Behav Biomed Mater 1:59–67. doi:10.1016/j.jmbbm.2007.04.001
4. Myllyharju J, Kivirikko KI (2004) Collagens, modifying enzymes and their mutations in humans, flies and worms. Trends Genet 20:33–43. doi:10.1016/j.tig.2003.11.004
5. Prockop DJ (1995) Collagens: molecular-biology, diseases, and potentials for therapy. Annu Rev Biochem 64:403–434. doi:10.1146/annurev.bi.64.070195.002155
6. Nalla RK, Stolken JS, Kinney JH, Ritchie RO (2005) Fracture in human cortical bone: local fracture criteria and toughening mechanisms. J Biomech 38:1517–1525. doi:10.1016/j.jbiomech.2004.07.010
7. Imbeni V, Kruzic JJ, Marshall GW, Marshall SJ, Ritchie RO (2005) The dentin-enamel junction and the fracture of human teeth. Nat Mater 4:229–232. doi:10.1038/nmat1323
8. Silva SS, Mano JF, Reis RL (2010) Potential applications of natural origin polymer-based systems in soft tissue regeneration. Crit Rev Biotechnol 30:200–221. doi:10.3109/07388551.2010.505561
9. Buehler MJ, Yung YC (2009) Deformation and failure of protein materials in physiologically extreme conditions and disease. Nat Mater 8:175–188. doi:10.1038/nmat2387
10. Mudera V, Morgan M, Cheema U, Nazhat S, Brown R (2007) Ultra-rapid engineered collagen constructs tested in an *in vivo* nursery site. J Tissue Eng Regen M 1:192–198. doi:10.1002/term.25
11. Kanungo BP, Silva E, Van Vliet K, Gibson LJ (2008) Characterization of mineralized collagen-glycosaminoglycan scaffolds for bone regeneration. Acta Biomater 4:490–503. doi:10.1016/j.actbio.2008.01.003
12. Barthelat F, Rabiei R (2011) Toughness amplification in natural composites. J Mech Phys Solids 59:829–840. doi:10.1016/j.jmps.2011.01.001
13. Fratzl P, Weinkamer R (2007) Nature's hierarchal materials. Prog Mater Sci 52:1263–1334. doi:10.1016/j.pmatsci.2007.06.001

14. Hulmes DJ, Wess TJ, Prockop DJ, Fratzl P (1995) Radial packing, order, and disorder in collagen fibrils. Biophys J 68:1661–1670. doi:10.1016/S0006-3495(95)80391-7
15. Diamant J, Keller A, Baer E, Litt M, Arridge RGC (1972) Collagen; ultrastructure and its relation to mechanical properties as a function of aging. Proc Roy Soc B - Biol Sci 180:293–315. doi:10.1098/rspb.1972.0019
16. Pins G, Silver F (1995) A self-assembled collagen scaffold suitable for use in soft and hard tissue replacement. Mat Sci Eng C - Biol S 3:101–107. doi:10.1016/0928-4931(95)00109-3
17. Sasaki N, Odajima S (1996) Stress–strain curve and young's modulus of a collagen molecule as determined by the X-ray diffraction technique. J Biomech 29:655–658. doi:10.1016/0021-9290(95)00110-7
18. Sasaki N, Odajima S (1996) Elongation mechanism of collagen fibrils and force-strain relations of tendon at each level of structural hierarchy. J Biomech 29:1131–1136. doi:10.1016/0021-9290(96)00024-3
19. Fratzl P, Misof K, Zizak I, Rapp G, Amenitsch H, Bernstorff S (1998) Fibrillar structure and mechanical properties of collagen. J Struct Biol 122:119–122. doi:10.1006/jsbi.1998.3966
20. Misof K, Rapp G, Fratzl P (1997) A new molecular model for collagen elasticity based on synchrotron x-ray scattering evidence. Biophys J 72:1376–1381. doi:10.1016/S0006-3495(97)78783-6
21. Yamamoto E, Hayashi K, Yamamoto N (1999) Mechanical properties of collagen fascicles from the rabbit patellar tendon. J Biomech Eng - T ASME 121:124–131. doi:10.1115/1.2798033
22. Puxkandl R, Zizak I, Paris O, Keckes J, Tesch W, Bernstorff S, Purslow P, Fratzl P (2002) Viscoelastic properties of collagen: synchrotron radiation investigations and structural model. Phil Trans R Soc B 357:191–197. doi:10.1098/rstb.2001.1033
23. Silver FH, Freeman JW, Seehra GP (2003) Collagen self-assembly and the development of tendon mechanical properties. J Biomech 36:1529–1553. doi:10.1016/S0021-9290(03)00135-0
24. Robinson PS, Lin TW, Reynolds PR, Derwin KA (2004) Strain-rate sensitive mechanical properties of tendon fascicles from mice with genetically engineered alterations in collagen and decorin. J Biomech Eng - T ASME 126:252–257. doi:10.1115/1.1695570
25. Currey JD (1984) Effects of differences in mineralization on the mechanical properties of bone. Phil Trans R Soc B 304:509–518. doi:10.1098/rstb.1984.0042
26. Gupta HS, Zioupos P (2008) Fracture of bone tissue: the 'hows' and the 'whys'. Med Eng Phys 30:1209–1226. doi:10.1016/j.medengphy.2008.09.007
27. Ikoma T, Kobayashi H, Tanaka J, Walsh D, Mann S (2003) Microstructure, mechanical, and biomimetic properties of fish scales from pagrus major. J Struct Biol 142:327–333. doi:10.1016/S1047-8477(03)00053-4
28. van der Rijt JAJ, van der Werf KO, Bennink ML, Dijkstra PJ, Feijen J (2006) Micromechanical testing of individual collagen fibrils. Macromol Biosci 6:697–702. doi:10.1002/mabi.200600063
29. Wenger MPE, Bozec L, Horton MA, Mesquida P (2007) Mechanical properties of collagen fibrils. Biophys J 93:1255–1263. doi:10.1529/biophysj.106.103192
30. Wenger MPE, Horton MA, Mesquida P (2008) Nanoscale scraping and dissection of collagen fibrils. Nanotechnology 19:384006. doi:10.1088/0957-4484/19/38/384006
31. Yang L, van der Werf KO, Koopman BFJM, Subramaniam V, Bennink ML, Dijkstra PJ, Feijen J (2007) Micromechanical bending of single collagen fibrils using atomic force microscopy. J Biomed Mater Res A 82A:160–168. doi:10.1002/jbm.a.31127
32. Yang L, van der Werf KO, Fitié CFC, Bennink ML, Dijkstra PJ, Feijen J (2008) Mechanical properties of native and cross-linked type I collagen fibrils. Biophys J 94:2204–2211. doi:10.1529/biophysj.107.111013
33. Svensson RB, Hassenkam T, Hansen P, Magnusson SP (2010) Viscoelastic behavior of discrete human collagen fibrils. J Mech Behav Biomed 3:112–115. doi:10.1016/j.jmbbm.2009.01.005
34. Eppell SJ, Smith BN, Kahn H, Ballarini R (2006) Nano measurements with micro-devices: mechanical properties of hydrated collagen fibrils. J R Soc Interface 3:117–121. doi:10.1098/rsif.2005.0100
35. Shen ZL, Dodge MR, Kahn H, Ballarini R, Eppell SJ (2008) Stress–strain experiments on individual collagen fibrils. Biophys J 95:3956–3963. doi:10.1529/biophysj.107.124602
36. Cusack S, Miller A (1979) Determination of the elastic constants of collagen by Brillouin light scattering. J Mol Biol 135:39–51. doi:10.1016/0022-2836(79)90339-5
37. Sun YL, Luo ZP, Fertala A, An KN (2002) Direct quantification of the flexibility of type I collagen monomer. Biochem Biophys Res Commun 295:382–386. doi:10.1016/S0006-291X(02)00685-X
38. Sun YL, Luo ZP, Fertala A, An KN (2004) Stretching type II collagen with optical tweezers. J Biomech 37:1665–1669. doi:10.1016/j.jbiomech.2004.02.028
39. Thompson JB, Kindt JH, Drake B, Hansma HG, Morse DE, Hansma PK (2001) Bone indentation recovery time correlates with bond reforming time. Nature 414:773–776. doi:10.1038/414773a
40. Bozec L, Horton M (2005) Topography and mechanical properties of single molecules of type I collagen using atomic force microscopy. Biophys J 88:4223–4231. doi:10.1529/biophysj.104.055228
41. Buehler MJ, Keten S, Ackbarow T (2008) Theoretical and computational hierarchical nanomechanics of protein materials: deformation and fracture. Prog Mater Sci 53:1101–1241. doi:10.1016/j.pmatsci.2008.06.002
42. Gautieri A, Buehler MJ, Redaelli A (2009) Deformation rate controls elasticity and unfolding pathway of single tropocollagen molecules. J Mech Behav Biomed 2:130–137. doi:10.1016/j.jmbbm.2008.03.001
43. Kaul PB, Singh U, Prakash V (2009) *In situ* characterization of nanomechanical behavior of free-standing nanostructures. Exp Mech 49:191–205. doi:10.1007/s11340-008-9179-4
44. Holbery JD, Eden VL, Sarikaya M, Fisher RM (2000) Experimental determination of scanning probe microscope cantilever spring constants utilizing a nanoindentation apparatus. Rev Sci Instrum 71:3769–3776. doi:10.1063/1.1289509
45. Sader JE (1998) Frequency response of cantilever beams immersed in viscous fluids with applications to the atomic force microscope. J Appl Phys 84:64–76. doi:10.1063/1.368002
46. Sader JE, Chon JWM, Mulvaney P (1999) Calibration of rectangular atomic force microscope cantilevers. Rev Sci Instrum 70:3967–3969. doi:10.1063/1.1150021
47. Burnham NA, Chen X, Hodges CS, Matei GA, Thoreson EJ, Roberts CJ, Davies MC, Tendler SJB (2003) Comparison of calibration methods for atomic-force microscopy cantilevers. Nanotechnology 14:1–6. doi:10.1088/0957-4484/14/1/301
48. Zhu D, Ortega CF, Motamedi R, Szewciw L, Vernerey F, Barthelat F (2011) Structure and mechanical performance of a "modern" fish scale. Adv Eng Mater Article first published online: 14 OCT 2011. doi:10.1002/adem.201180057
49. Lemaître J (1996) A course on damage mechanics. Springer, New York